fermentation

MDPI

Article

Anti-Inflammatory and Osteogenic Effects of Vitamin K from *Sargassum fulvellum* Fermented by *Lactococcus lactis* KCCM12759P and *Leuconostoc mesenteroides* KCCM12756P

Yejin Sim [1,†], Hyun-Sol Jo [1,†], Choong-Gon Kim [2], Young-Eun Cho [3], Jungwoo Yang [4] and Sun-Mee Hong [1,*]

[1] Marine Industry Research Institute for East Sea Rim, 22 Haeyanggwahak-gil, Jukbyeon, Uljin-gun 36315, Republic of Korea; yejin5879@mire.re.kr (Y.S.); hyunsoljo@mire.re.kr (H.-S.J.)
[2] Marine Ecosystem Research Center, Korea Institute of Ocean Science and Technology, 385 Haeyang-ro, Yeongdo-go, Busan 49111, Republic of Korea; kimcg@kiost.ac.kr
[3] Department of Food and Nutrition, Andong National University, Andong 36729, Republic of Korea; yecho@anu.ac.kr
[4] Department of Microbiology, College of Medicine, Dongguk University, Gyeongju 38066, Republic of Korea; dbl3jwy@dongguk.ac.kr
* Correspondence: hongsunmee@mire.re.kr; Tel.: +82-54-780-3461; Fax: +82-54-780-3469
† These authors contributed equally to this work.

Abstract: Vitamin K (VitK) is a vital nutrient that is newly recognized to support bone and cardiovascular health. As a nutraceutical, VitK is produced via plant extraction and bacterial fermentation. This study examined the potential anti-inflammatory and osteogenic benefits of VitK, i.e., VitK1 (phylloquinone; PK) and VitK2 (menaquinone; MKs), derived from *Sargassum fulvellum* fermented by *Lactococcus lactis* and *Leuconostoc mesenteroides* (SfLlLm) using lipopolysaccharide (LPS)-induced Raw264.7, MC3T3-E1 cells, and ovariectomized (OVX) mice. MK4, MK7, and MK9, as well as PK, were effectively acquired from SfLlLm and analyzed. SfLlLm_VitK reduced levels of proinflammatory cytokine in LPS-induced Raw264.7 cells and induced an osteogenesis regulating factor in MC3T3-E1 cells. In OVX mice, SfLlLm feeding reduced plasma levels of alkaline phosphatase, phosphate, and the pro-collagen type I alpha 2 gene (pro-Col1a2) while elevating cancellous bone volume and trabecular numbers. Accordingly, SfLlLm, comprising MKs, may be a candidate for preventing and treating immune and bone diseases.

Keywords: lactic acid bacteria; *Sargassum* sp.; menaquinone; inflammation; osteogenesis

Citation: Sim, Y.; Jo, H.-S.; Kim, C.-G.; Cho, Y.-E.; Yang, J.; Hong, S.-M. Anti-Inflammatory and Osteogenic Effects of Vitamin K from *Sargassum fulvellum* Fermented by *Lactococcus lactis* KCCM12759P and *Leuconostoc mesenteroides* KCCM12756P. *Fermentation* **2024**, *10*, 569. https://doi.org/10.3390/fermentation10110569

Academic Editor: Penka Petrova

Received: 10 October 2024
Revised: 1 November 2024
Accepted: 5 November 2024
Published: 7 November 2024

1. Introduction

Algae form the basis of the food chain and cover more than 70% of the world's total living mass. *Sargassum fulvellum* (*S. fulvellum*) is popular and inexpensive edible brown seaweed enriched in nutrients, such as carbohydrates, lipids, proteins, vitamins, and minerals, and is also a source of several health-promoting components, including fucoxanthin, phlorotannins, and polysaccharides [1]. Currently, owing to the growing demand for vitamins as market leaders for high-value bioproducts, algae-derived vitamins are gaining traction for applications in food, feed, cosmetic, chemical, and pharmaceutical industries. Vitamins, essential micro-nutrients for life, are either not or minimally synthesized in animals and humans, thus necessitating continuous assimilation through diet intake of plants, fruits, or seeds [2]. Most vitamins are synthesized by photosynthetic organisms, whereas vitamins B and K are bioaccumulated through the diet and are mainly produced by bacteria [3]. For use as nutraceutical and dietary supplements, large-scale vitamin production is currently accomplished through chemical synthesis, extraction from natural sources, and microbial fermentation [4]. Given the health benefits of vitamin K (VitK) and increasing consumer preference for natural products, there is a clear need to identify sustainable and cost-effective methods for producing natural-derived VitK. Notably, VitK

exists mainly in two natural forms: VitK1 (phylloquinone; PK), which is present in plants and algae, and VitK2 (menaquinone; MKn or MKs), which is present in animal foods (MK4) or synthesized by microorganisms (MK5 to MK13) [5]. MKs, including MK7 and MK9, are bacterial products found in fermented foods, such as natto and chenggukjang produced by *Bacillus subtilis* and cheese by *Lactoccocus* ssp. [6–8]. PK and MKs play multifunctional roles in a wide range of biological activities, including blood coagulation, bone maintenance, the prevention of arterial hardening, neuroprotection, and the modulation of inflammation [9–12]. Recently, the importance of vitamin K, calcium, and vitamin D has been highlighted in the prevention and treatment of osteoporosis [13,14] (Villa et al., 2017; Capozzi et al., 2020).

In silico studies revealed that lactic acid bacteria (LAB) genomes encode the complete menaquinone biosynthesis pathway in *Lactococcus lactis* (*L. lactis)* and *Leuconostoc mesenteroides* (*L. mesenteroides*) [15,16]. Previously, we reported and selected *L. lactis* (KCCM12759P) with menA–F, menH, menI, and *L. mesenteroides* (KCCM12756P) with menB, menE, and menG, isolated from the East Sea of the Republic of Korea, which produced MKs and inhibited vascular calcification [17].

Osteoporosis, a systemic skeletal disease, is characterized by bone mass reduction and microstructural deterioration of the bone tissue. Osteoporosis has been associated with age and the deficiency of sex hormones (estrogen, testosterone) [18], in addition to causes such as various inflammatory diseases and drugs [19]. Among the various mechanisms, the correlation between osteoporosis and inflammatory cytokines has been established. Owing to its anatomical characteristics, bone tissue is closely related to the immune system, both internally and externally. Immunostained cells function collaboratively within the bone marrow to induce hematopoiesis, as well as outside the skeleton, leading to joint destruction and chronic inflammatory joint disease [20,21]. Well-known osteoimmune system molecules include RANKL (the receptor activator of nuclear factor kappa B ligand), interleukin (IL)-1, IL-6, IL-8, the tumor necrosis factor (TNF)-α, and Dickkopf-1 (Dkk-1), which play pivotal roles in bone growth and remodeling and bone metastases in osteoblasts, preosteoblasts, osteoclasts, and macrophages [21].

This study focused on long-chain MKs, given that they are produced via algae- and LAB-based fermentation and could exert immune and bone health benefits compared with algae-based VitK forms. The objective of the current study was to provide insights into the natural MK production capacities of L. lactis and L. mesenteroides and the influence of S. fulvellum nutrients, including PK, on MK production. Initially, the MK forms and quantity produced by the co-culture of L. lactis and L. mesenteroides with S. fulvellum were determined. Then, the anti-inflammatory and osteogenic effects of the obtained VitK were analyzed in LPS-treated RAW264.7 cells, MC3T3-E1 preosteoblasts, and ovariectomized (OVX) mice.

2. Materials and Methods

2.1. Preparation of S. fulvellum Extract and Fermentation

S. fulvellum was purchased from Parajeju (http://www.parajeju.com), dried, ground, and autoclaved to prepare 5% Sf media (*w*/*v* in distilled water; Sf) before fermentation. In previous studies, LAB *L. lactis* (Ll, KCCM12759P) and *L. mesenteroides* (Lm, KCCM12756P) were isolated from the East Sea of the Republic of Korea and selected to produce menaquinone (VitK2; MKs) using genomic PCR using menA~G gene primers [16,17]. Ll and Lm were precultured individually in deMan, Rogosa, and Sharpe (MRS) broth at 30 °C for 24 h to 1 × 10^9 CFU/mL. Then, 1% LlLm (equal volumes of each Ll and Lm culture) was inoculated in 5% Sf media and cultured at 30 °C for 24 h to 1 × 10^{10}~1 × 10^{11} CFU/mL and then lyophilized (SfLlLm) or used for VitK analysis.

2.2. VitK Analysis

The extraction and analysis of VitK1 and MKs in Sf and SfLlLm were performed using an established procedure with modifications [22]. In brief, 10 g of Sf and SfLlLm

(pellets collected from 200 mL of media after centrifugation) were mixed with 25 mL of n-hexane and 2-propanol (2:1; *v*/*v*) by vortexing, and the liquid layer was collected. The pellet was then remixed, and 25 mL of 2-propanol was collected by performing the same procedure three times. The organic phase was evaporated and concentrated to 10 mL using a nitrogen evaporator (Infitek, Jinan, China). After filtering through a 0.45 μm filter (Millipore, Burlington, MA, USA), each sample was detected by performing HPLC (Shimadzu Prominence HPLC system, Kyoto, Japan) LC/MS/MS (API 5500 QTRAP; AB SCIEX, Framingham, MA, USA). A Kinetex C18 column (Phenomenex, Torrance, CA, USA) was used, and the temperature was maintained at 60 °C. Mobile phase A comprised 5 mM of ammonium formate with 0.1% formic acid, while mobile phase B comprised 5 mM of ammonium formate with 0.1% formic acid in isopropanol and methanol (9:1; *v*/*v*; Merck, Darmstadt, Germany). The flow rate was 0.5 mL/min, and the injection volume of the sample was 5 μL. The peaks were detected at 320 and 430 nm using a fluorescence detector and using standards of PK (MW 450.7 g/mol; Sigma, Burbank, CA, USA), MK4 (MW 444.6 g/mol; Sigma, USA), MK7 (MW 649 g/mol; Sigma, USA) and MK9 (MW 785.2 g/mol; Sigma, USA). The PK and MK concentrations were quantified by comparing the obtained standard values with sample values.

2.3. Antioxidant Analysis

First, the free radical scavenging activity of Sf and SfLlLm was determined using the representative DPPH assay (Sigma, USA) correlated with the ABTS and FRAP assay of the antioxidant. In 96-well microplates, 30 μL of a sample solution and 70 μL of DPPH solution (0.2 mM in methanol) were added and reacted for 30 min under dark conditions. After the reaction, the optical density (OD) was measured at 517 nm using a microplate reader (Thermo Fisher Scientific, Waltham, MA, USA). The percentage inhibition was calculated as follows:

$$\text{DPPH radical scavenging activity (\%)} = \{1 - (\text{OD sample}/\text{OD blind})\} \times 100$$

where the OD sample and the OD blind are the absorbance values of the sample and non-sample, respectively. Superoxide anion scavenging activity was determined using the SOD Assay Kit-WST, according to the manufacturer's protocol (Dojindo, Kumamoto, Japan). Briefly, 10 μL of a sample was added to the well of a 96-well microplate, followed by the addition of a 200 μL WST working solution and a 20 μL enzyme working solution. Subsequently, the reaction mixture was incubated at 37 °C for 20 min, and absorbance was measured at 450 nm using a microplate reader (Thermo, USA).

The percentage of inhibition was calculated as follows:

$$\text{Superoxide dismutase (SOD) activity (\%)} = \{1 - (\text{OD sample}/\text{OD blind})\} \times 100$$

where the OD sample and the OD blind are the absorbance values of the sample and non-sample, respectively. Ascorbic acid (100 mg/mL; Sigma, USA) was used as a positive control, and the equations for the DPPH and SOD activity were calculated.

2.4. Cell Culture and Differentiation

RAW264.7 cells, a macrophage cell line, were purchased from Korean Cell Line Bank (KCLB, Seoul, Korea) and cultured in a Dulbecco Modified Eagle Medium (Gibco, Waltham, MA, USA), supplemented with a 10% fetal bovine serum (FBS; *v*/*v*; Gibco, USA) and 1% penicillin/streptomycin (*v*/*v*) at 37 °C in a humidified incubator with a 5% CO_2 atmosphere. MC3T3-E1 cells, a murine preosteoblastic subclone 4 cell line, were purchased from the American Type Culture Collection (ATCC, Manassas, VA, USA) and incubated in alpha minimum essential medium (Gibco, USA), supplemented with a 10% FBS (*v*/*v*) and 1% penicillin/streptomycin (*v*/*v*) in the same incubator as Raw264.7 cells. To assess the effects on differentiation, after reaching 80% confluency, the cell medium was replaced with a complete differentiation medium (DM) containing 10 mM of β-glycerophosphate (Sigma,

USA) and 100 μg/mL of ascorbic acid (Sigma, USA). After treatment with Sf and SfLlLm, the medium was changed every three days, and the cells were harvested on days 3 and 7.

2.5. Cell Viability

Cytotoxicity was determined using the Cytotoxicity LDH Assay Kit-WST (Dojindo, Seoul, Korea), as described in the manufacturer's protocol. Briefly, RAW264.7 and MC3T3-E1 cells were seeded in 96-well microplates at a density of 5×10^4 cells/mL after washing the cells twice with a phosphate-buffered saline (PBS). The cells were then cultured for 24 h with a cell medium containing different concentrations of Sf and SfLlLm (0, 280, 560, and 840 ng/mL). The toxicity of Sf and SfLlLm was measured at 450 nm using a microplate reader (Thermo, USA). Raw264.7 and MC3T3 cells were used as control macrophages and preosteoblasts, respectively.

2.6. Nitric Oxide (NO) Determination

Briefly, RAW264.7 cells (1×10^5 cells/mL) were treated with 1 μg/mL lipopolysaccharide (LPS; Sigma, USA) for 1 h. Subsequently, LPS was removed, and cells were incubated with various concentrations of Sf and SfLlLm (0, 280, 560, and 840 ng/mL) for 24 h. The NO level in the cell culture medium was detected using a NO assay kit (Dogendo, Seoul, Korea) at 540 nm. The cell pellets were collected, centrifuged at 8000 rpm for 10 min, and stored at −80 °C until further analysis.

2.7. Alkaline Phosphatase (ALP) Assay

ALP activity was determined using an Alkaline Phosphatase Detection Kit (Merck, Rahway, NJ, USA). Briefly, MC3T3-E1 cells were seeded at a density of 1×10^4 cells/mL in 12-well plates and treated with various concentrations of Sf and SfLlLm (0, 280, 560, and 840 ng/mL) for three or seven days. The culture medium was collected, and the cells were washed twice with a cold PBS before detachment, followed by lysis in a solution of Triton X-100 and 1× assay buffer. The collected medium and lysed cells were transferred to 96-well plates, and a colorimetric 50 μL ALP substrate was added. The plate was incubated for 10 min at 37 °C in a humidified incubator with a 5% CO_2 atmosphere, and the absorbance was measured at 405 nm using a microplate reader (Thermo, USA). ALP activity was calculated as follows: activity (%) = (OD sample/OD control) × 100. MC3T3 cells were used as the control preosteoblasts.

2.8. Osteoblast Mineralization Staining

To confirm the mineralization of the extracellular matrix, MC3T3-E1 cells were seeded (1×10^4 cells/mL) in 12-well plates and cultured in a DM containing Sf and SfLlLm (280, 560, and 840 ng/mL) for 3 and 7 days. Cells in each group were fixed with a 4% paraformaldehyde solution (Sigma, USA) for 15 min and then gently washed three times with distilled water.

For Alizarin Red S staining, the fixed cells were stained with 40 mM Alizarin Red S (pH 4.2) for 30 min at room temperature (RT) and washed three times. Stained cells were observed under an optical microscope. To quantify Alizarin Red S staining, the stained cells were lysed using 10% (*w*/*v*) cetylpyridinium chloride in 10 mM of sodium phosphate (pH 7.0) for 15 min. The cell lysate supernatant was transferred to 96-well plates and quantified using a plate reader at an absorbance of 570 nm [23].

To perform the von Kossa staining, fixed cells were stained with 5% silver nitrate (Sigma, USA), incubated for 1 h under UV light at RT, then washed with distilled water, and observed using an optical microscope. Mineralized nodules appeared as thick, dark, dark-brown stripes. MC3T3-E1 cells with and without DM treatment were used as negative and positive controls, respectively, and PK, MK4, MK7, and MK9 cells were used as reference controls.

2.9. Immunoblot Analysis

Both Raw264.7 and MC3T3 cells were seeded in 60 mm plates (3×10^5 cells/mL). Cells treated with and without Sf and SfLlLm were washed twice with 1× PBS and then homogenized using 1× RIPA buffer (Thermo, USA). Cell lysates were centrifuged at 12,000× *g* for 10 min at 4 °C. The protein concentration in the supernatant was quantified using a bicinchoninic acid protein assay kit (TaKaRa, Kyoto, Japan). Samples of equal protein concentration (50 μg of protein equally pooled from cells) were separated by sodium dodecyl sulfate-polyacrylamide gel electrophoresis (SDS-PAGE) and transferred to nitrocellulose membranes. The membranes were blocked with 5% skim milk prepared in tris-buffered saline containing 0.05% tween-20 (TBST) for 1 h, followed by overnight incubation with primary antibodies at 4 °C. The primary antibodies included inducible NO synthase (iNOS; Invitrogen, Carlsbad, CA, USA); cyclooxygenase-2 (COX-2; Invitrogen, USA), the receptor activator of nuclear factor κB ligand (RANKL; Cell Signaling, Danvers, MA, USA), interferon-gamma (IFN-γ; Cell Signaling), IL-1β (Cell Signaling), DKK-1 (Cell Signaling), TNF-α (Cell Signaling), and IL-6 (Cell Signaling) as proinflammation markers; ALP (Santa Cruz Biotechnology, Inc., Dallas, TX, USA), RUNX family transcription factor 2 (RUNX2; Santa Cruz Biotechnology), pro-collagen type I alpha 2 chain (pro-COL1A2; Santa Cruz Biotechnology), collagen type I alpha 1 (COL1A; Santa Cruz Biotechnology), and osteopontin (OPN; Santa Cruz Biotechnology) were used as osteogenesis expression markers. Glyceraldehyde 3-phosphate dehydrogenase (GAPDH; Cell Signaling) and β-actin (Cell Signaling) were used as loading control antibodies. After washing with TBST for 1 h, the membrane was incubated with a horseradish peroxidase (HRP)-conjugated anti-rabbit/mouse IgG secondary antibody for 1 h at RT. Finally, antibody binding was detected using a chemiluminescent Western blot reagent (ThermoFisher, USA), and the bands were visualized using the Invitrogen iBright Imaging System (ThermoFisher, USA). The band intensities were analyzed using iBright analysis software 21 CFR Part 11 (Thermo Fisher Scientific, USA), with GAPDH and β-actin used as loading controls.

2.10. Ethics Statement

The OVX-induced osteoporosis mouse model and all subsequent experimental protocols were reviewed and approved by the Ethics Committee of Andong University.

2.11. Construction of an OVX Animal Model

First, 20 C57BL/6 female mice (8-week-old; Orient Bio Inc., Korea) were randomly divided into four groups (n = 5 mice/group): sham (control; CONT), OVX (negative control; nCONT), OVX + 10% Sf, and OVX + 10% SfLlLm group. After the induction of anesthesia using tribromoethanol, the groups were separately subjected to sham surgery without ovariectomy or bilateral ovariectomy to induce osteoporosis. Two weeks after the operation, the sham and OVX groups received normal AIN-76A feed, whereas OVX + 10% Sf and OVX + 10% SfLlLm groups were provided AIN-76A feed, including 10% Sf and 10% SfLlLm, respectively, for 8 weeks. Subsequently, all mice were sacrificed, and plasma, femurs, and tibiae were harvested. The excess tissue was removed for micro-computed tomography (micro-CT) and histological assessments.

2.12. Micro-CT Analysis

After eight weeks, femur bones from each mouse were collected and scanned using a micro-CT system (Quantum FX, Perkin Elmer, Waltham, MA, USA). To determine conventional indices of bone structure, 120 Masson-Goldner-stained (Merck, USA) slices with a voxel size of 9.7 μm thick sections over the growth plate of the distal femur were evaluated. The cancellous bone volume (BV/TV) and trabecular number (Tb. N) were derived from three-dimensional reconstruction (sigma = 1.2, threshold, Th = 180, and support = 2): BV, bone volume; TV, tissue volume; and Tb, trabecular thickness [24].

2.13. Plasma Biochemical Marker Analysis

To detect plasma levels of indicators related to bone metabolism, plasma samples were analyzed using ELISA kits for ALP (Merck), phosphatase (Abcam, Waltham, MA, USA), and proCOL1α1 (Abcam, USA) according to the manufacturer's protocol. The absorbance of each sample was measured by using a spectrophotometer (Thermo Fisher Scientific).

2.14. Statistical Analysis

Data analyses were performed using the IBM SPSS 27.0 for Windows (IBM Corp., Armonk, NY, USA). The results are expressed as mean ± standard deviation (SD). Statistical significance was set at $p < 0.05$, using Duncan's multiple-range test.

3. Results and Discussion

3.1. VitK Identification in Sf and SfLlLm and the Antioxidant Effect

The Sf- and SfLlLm-derived PK and MKs used for in vitro and in vivo experiments were prepared and identified as shown in Figure 1A. To develop fermented *S. fulvellum* with high PK and MK contents, *L. lactis* and *L. mesenteroides* strains with male genes were co-inoculated in 5% Sf media for MK production (Figure 1A; [17]. To enhance the MK content of Sf with natural PK, Sf was fermented with both LAB at 30 °C after 24 h (SfLlLm) and extracted with isopropanol; then, the PK and MK contents were measured. Figure 1B presents the Sf content of PK (1045.13 ± 2.37 μg/100 g), MK4 (382 ± 24.97 μg/100 g), and the SfLlLm contents of PK (1057.32 ± 2.66 μg/100g), MK4 (327.86 ± 24.86 μg/100 g), MK7 (11.81 ± 0.20 μg/100 g), and MK9 (2.70 ± 0.21 μg/100 g). Although only MK4 was detected in the Sf medium, SfLlLm contained quantities of PK comparable to those present in Sf, along with MK forms ranging from MK4 to MK9 (Figure 1B). Morishita et al. reported that *L. lactis* and *L. mesenseeroides* produce MKs [25]. However, to the best of our knowledge, this study is the first to produce long-chain MKs through co-culture.

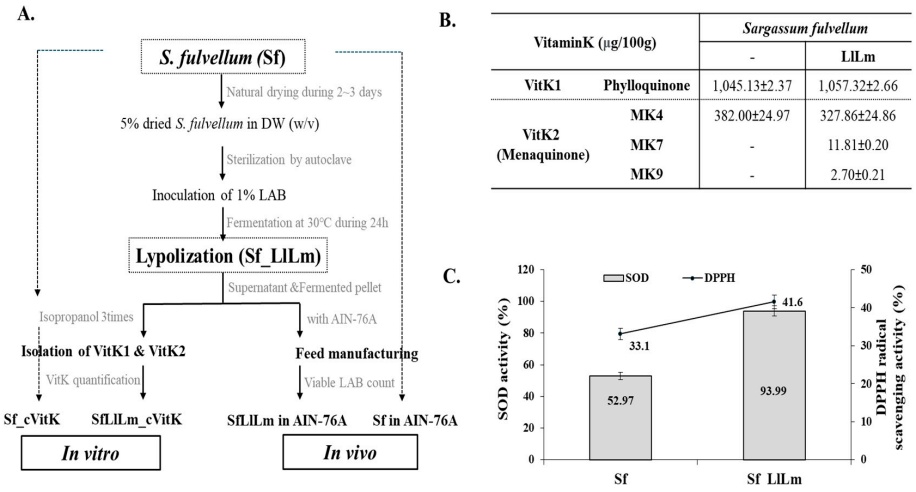

VitaminK (μg/100g)		*Sargassum fulvellum*	
		-	LlLm
VitK1	Phylloquinone	1,045.13±2.37	1,057.32±2.66
VitK2 (Menaquinone)	MK4	382.00±24.97	327.86±24.86
	MK7	-	11.81±0.20
	MK9	-	2.70±0.21

Figure 1. Preparation, antioxidant assessment, and quantification of vitamin K from Sf and SfLlLm: (**A**) Flowchart of sample preparation from *S. fulvellum* for in vitro and in vivo assessments. (**B**) Identification and quantification of VitK1 and VitK2 (MKs) produced from Sf and SfLlLm by HPLC. (**C**) Antioxidant effects determined using DPPH and SOD assays. Data are represented as the means ± standard deviation of three independent experiments. MKs, menaquinones; SOD, superoxide dismutase; VitK, vitamin K.

Oxidative stress is considered an important biological factor in osteoporosis [26]. Herein, DPPH and SOD assays were performed to evaluate the antioxidant activities of Sf and SfLlLm. The SfLlLm showed high DPPH and SOD activities, i.e., 93.99 and 41.6%, respectively, which were significantly greater than those of the Sf (52.97 and 33.1%, respectively; Figure 1C). These results suggest that SfLlLm, including MKs, may help prevent or treat osteoporosis and bone inflammatory diseases.

3.2. Inflammatory Effect in LPS-Induced Raw264.7 Cells

To determine the effects of Sf and SfLlLm with complex VitK (PK and MKs) on cell viability, Raw264.7 macrophage cells were treated with the isolated Sf_cVitK and SfLlLm_cVitK (Figure 1A,B) at different concentrations ranging from 0, 280, 560, and 840 ng/mL for 24 h. Based on the results of the lactate dehydrogenase (LDH) assay, no cytotoxic effects were observed at the concentrations used in this study ($p < 0.01$; Figure 2A). Subsequently, these non-toxic concentrations were used to determine potential anti-inflammatory effects. The capacities of Sf_cVitK and SfLlLm_cVitK to regulate the LPS-stimulated inflammatory response of macrophages were determined. ELISA was performed to detect NO levels in the supernatants of LPS-induced cells treated with different concentrations of Sf_cVitK or SfLlLm_cVitK. Treatment with both Sf_cVitK and SfLlLm_cVitK, respectively, potently suppressed the LPS-induced production and secretion of NO (Figure 2B) in a concentration-dependent manner. Based on our observation of the NO inhibition in the supernatants of LPS-induced Raw264.7 cells, Sf_cVitK and SfLlLm_cVitK may suppress the activation of cytokines related to bone remodeling following LPS stimulation [21]. Accordingly, immunoblot analysis was performed to confirm whether Sf_cVitK and SfLlLm_cVitK suppressed iNOS, COX2, IL1β, TNF-α, IL-6, IFN-γ, DKK-1, and RANKL in LPS-induced cells (Figure 2C). Notably, treatment with SfLlLm_cVitK significantly inhibited the LPS-induced degradation of the eight cytokines in a concentration-dependent manner, and this effect was greater than that observed upon treatment with Sf_cVitK (Figure 2C). The treatment of LPS-induced cells with SfLlLm_cVitK for 24 h significantly reduced the levels of four major inflammatory factors, IL1β, TNF-α, IFN-γ, and DKK-1 ($p < 0.01$; Figure 2D). These data verified that SfLlLm_cVitK could regulate the LPS-induced production of NO and cytokines when compared with Sf_cVitK. Reportedly, MKs can downregulate basal and cytokine-induced NF-κB activation in human and murine monocytic cell lines, thereby preventing bone resorption [27]; these effects are triggered by the side chains of MKs but not by PK side chains [28]. These findings support the possibility that MKs produced from SfLlLm can suppress inflammation in LPS-induced Raw264.7 cells.

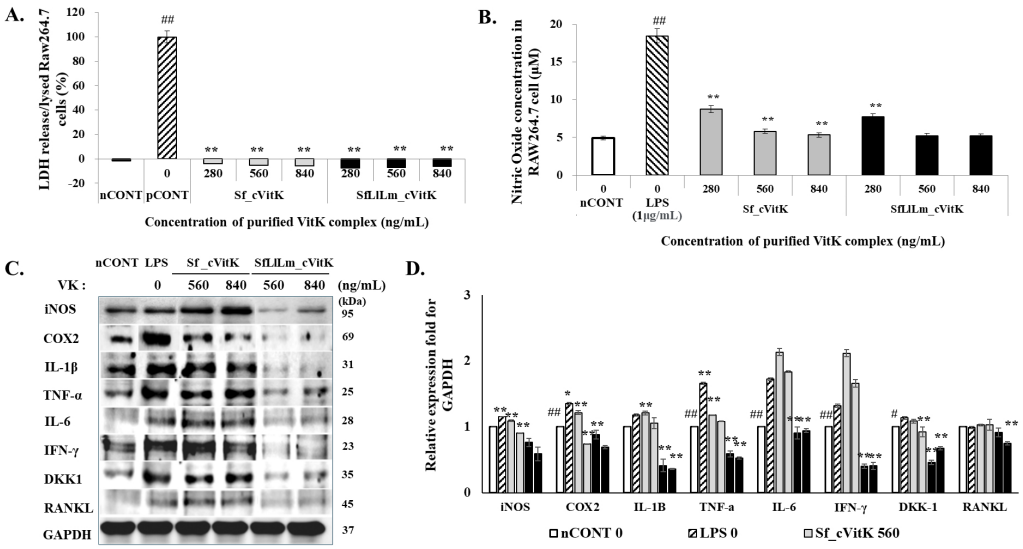

Figure 2. Anti-inflammatory effects of VitK isolated from nonfermented and fermented *S. fulvellum* in LPS-stimulated Raw264.7 cells: (**A**) Cell cytotoxicity by LDH assay. (**B**) Nitric oxide inhibition effects by Griess reaction assay. (**C**) Immunoblotting analysis for the expression of eight cytokines, iNOS, COX-2, IL-1β, TNF-α, IL-6, IFN-γ, DKK-1, and RANKL. (**D**) Relative expression levels of six cytokines compared with GAPDH. Data are represented as the means ± standard deviation of three independent experiments, ## $p < 0.01$ vs. Control group, and * $p < 0.05$ and ** $p < 0.01$ vs. LPS group. COX-2, cyclooxygenase-2; DKK-1, Dickkopf-1; iNOS, inducible nitric oxide; IFN-γ, interferon-gamma, IL-1β, interleukin-1β; IL-6, interleukin-6; LDH, lactate dehydrogenase; LPS, lipopolysaccharide; TNF-α, tumor necrosis factor-α; RANKL, receptor activator of nuclear factor κB ligand; VitK, vitamin K.

3.3. Effects of Osteogenic Activation and Mineralization in MC3T3-E1 Cells

The effects of Sf_cVitK and SfLlLm_cVitK on the cytotoxicity, differentiation, and mineralization in MC3T3-E1 preosteoblastic cells were determined. In the LDH assay, MC3T3 cells treated with Sf_cVitK and SfLlLm_cVitK showed non-cytotoxicity up to 840 ng/mL for up to 7 days ($p < 0.05$; Figure 3A). ALP levels in the medium were slightly increased in MC3T3-E1 cells treated with 560 or 840 ng/mL Sf_cVitK and SfLlLm_cVitK at 3 days when compared with those in control but were normalized at 7 days ($p < 0.05$ and $p < 0.01$, respectively; Figure 3B). The ALP concentration in the medium was similar to that in the control cells. In the bone, ALP, a marker of osteogenic differentiation of bone cells and mineralized matrix deposition, w released into the serum through matrix vesicles or after cleavage from the osteoblast surface [29]. ALP is present in the serum and can be used as a biomarker of bone disorders [30]. The normalized ALP concentration in the medium indicated a normal stimulation of osteoblast differentiation or extracellular matrix mineralization in Sf_cVitK- or SfLlLm_cVitK-treated MC3T3-E1 cells.

Next, to characterize the biological mineralization of Sf_cVitK and SfLlLm_cVitK, Von Kossa and Alizarin red S staining examinations were performed, and the respective levels were measured (Figure 3C,D). Von Kossa staining can detect calcium anions (such as phosphate and sulfates) in the osteoblastic cellular matrix, whereas Alizarin Red S staining can visualize calcium cation chelates [31]. In Von Kossa and Alizarin red S staining assessments, using PK and MKs as the reference control, staining intensity was increased in mineralized nodules 7 days after treatment with 1 μg/mL of MK4 and MK9, respectively, with weak intensity observed upon treatment with PK and MK7. In both staining analyses, calcium deposits, as bone mineralization markers, were dose-dependently increased in Sf_cVitK- and SfLlLm_cVitK-treated MC3T3-E1 cells after 7 days (Figure 3C). The quantitative analysis of calcium deposition by Alizarin Red S staining revealed that the concentration of Ca-mineralized nodules was increased in Sf_cVitK- or SfLlLm_cVitK-treated MC3T3-E1 cells in a dose-dependent manner (Figure 3D). Based on von Kossa and Alizarin Red S staining, treatment with PK and MK7 (reference controls) resulted in lower calcium deposition, whereas higher calcium levels were detected with MK4 and MK9 treatment (Figure 3C,D). According to LC-MS/MS analysis, similar to SfLlLm_cVitK, Sf_cVitK contained MK4 but not MK7 or MK9 (Figure 1B). Overall, Sf_cVitK, which comprised PK and MK4, could promote the differentiation and mineralization of preosteoblastic MC3T3-EL cells when compared with SfLlLm_cVitK, which comprised PK, MK4, MK7, and MK9. These results suggest that MK4 present in Sf and SfLlLm likely stimulates the differentiation and mineralization of preosteogenic MC3T3-E1 cells. Additionally, MK7, as an MK4 precursor, may be superior to MK4 itself to achieve MK4-specific physiological effects.

To further elucidate potential pathways through which Sf_cVitK and SfLlLm_cVitK stimulate osteoblast differentiation in MC3T3-E1 cells, the protein expression levels of ALP, pro-Col1A2, Col1A2, Runx2, and OPN, well-known bone remodeling markers, were analyzed by immunoblotting (Figure 3E,F). As shown in Figure 3E, ALP, pro-Col1A2, Col1A2, and the Runx2 protein, which are expressed by preosteoblasts, bone-forming cells, and mature osteoblasts, were upregulated in MC3T3-E1 cells treated with 560 or 840 ng/mL of Sf_cVitK and SfLlLm_cVitK in a dose-dependent manner at 7 days ($p < 0.01$ or $p < 0.05$), although the levels were only slightly promoted in SfLlLm_cVitK-treated MC3T3-E1 cells when compared with those in Sf_cVitK-treated cells. Conversely, the expression of OPN, a protein involved in osteoclast attachment to the mineralized bone matrix and a bone matrix protein, was unaltered when compared with that in non-treated MC3T3-E1 cells. Furthermore, SfLlLm_cVitK significantly increased the expression of proteins associated with osteoblast proliferation and differentiation, including ALP, pro-Col1A2, and Runx2, in MC3T3-E1 cells (Figure 3F). These results indicated that SfLlLm_cVitK may stimulate bone differentiation more than Sf_cVitK, potentially promoting osteoblastogenesis in MC3T3-E1 cells. In MC3T3-E1 cells, Sf_cVitK and SfLlLm_cVitK could function as potential components that influence osteoblast- and osteocyte-related bone remodeling processes. VitK (PK and MKs) produced by the fermentation of Sf by LAB were consistent

with those obtained in previous studies [32], correlating with MKs capable of enhancing osteoblast differentiation and mineralization.

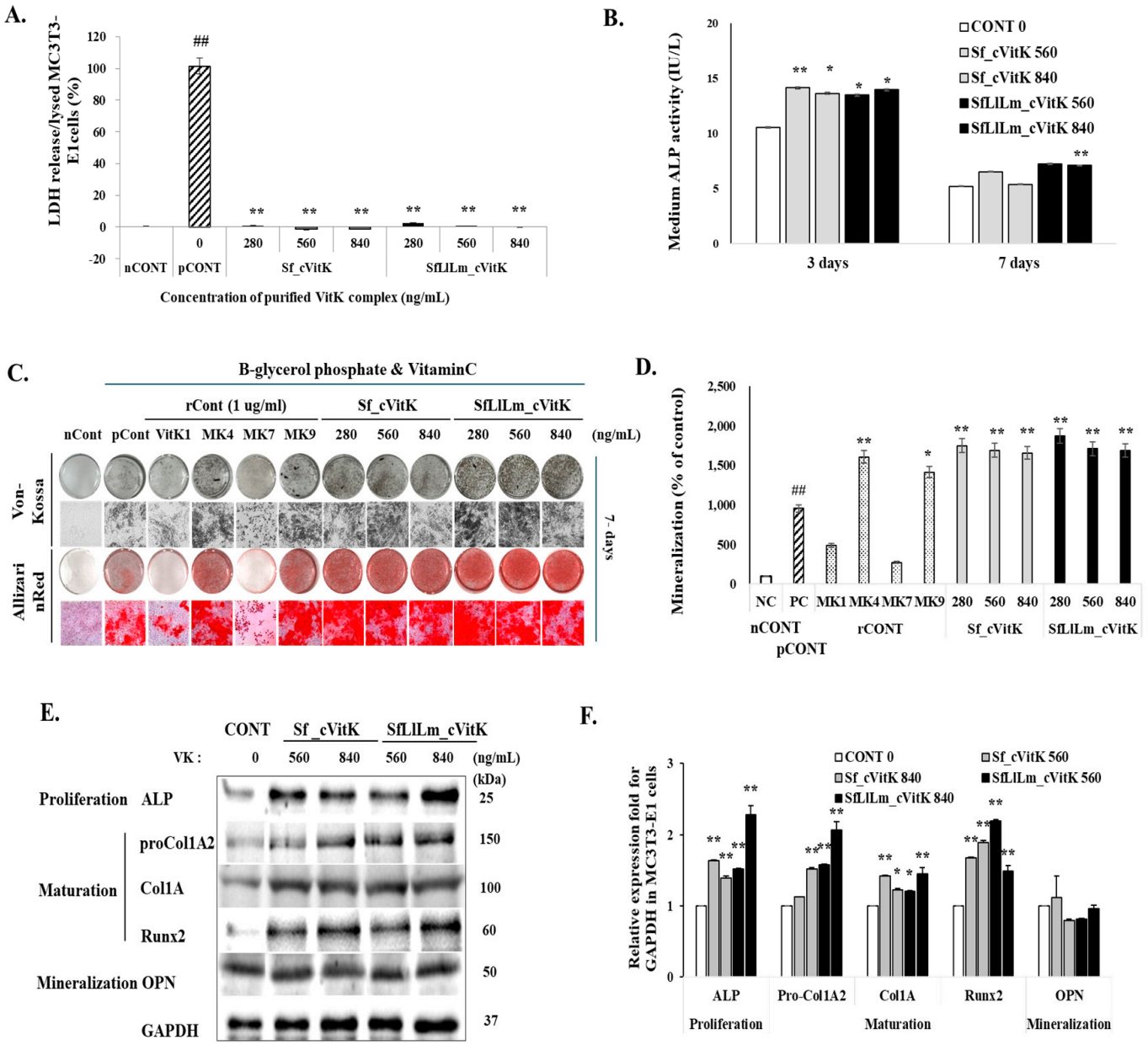

Figure 3. Preosteoblast differentiation and mineralization effects of VitK isolated from Sf and SfLlLm in MC3T3-E1 cells: (**A**) Cell cytotoxicity determined by LDH assay at 7 days. (**B**) ALP activity in cell medium at 3 and 7 days. (**C**) Von-Kossa and Alizalin Red-S staining to visualize mineralization at 7 days. (**D**) The relative quantitative value of stained cells compared with non-treated cells using a phase-contrast microscope. (**E**) Immunoblotting analysis for the protein expression of ALP, pro-Col1A2, Col1A2, Runx2, and OPN. (**F**) The relative expression of ALP, pro-Col1A2, Col1A2, Runx2, and OPN compared with GAPDH. Data are represented as mean ± standard deviation of three independent experiments, ## $p < 0.01$ vs. Control group, and * $p < 0.05$ and ** $p < 0.01$ vs. positive Control group. ALP, alkaline phosphatase; LDH, lactate dehydrogenase; RUNX2, RUNX family transcription factor 2; pro-COL1A2, pro-collagen type I alpha 2 chain; COL1A, collagen type I alpha 1; OPN osteopontin; VitK, vitamin K.

3.4. Effects of Sf and SfLlLm in OVX Mice

Next, the preventive effect of fermented sargassum-derived VitK (PK and MKs) on OVX-induced bone loss was examined in 8-week-old female mice. Experimental mice were fed a normal diet (AIN-76A) and an AIN-76A comprising 10% Sf and 10% SfLlLm (Sf and SfLlLm) for 8 weeks, starting two weeks before OVX or sham surgery (Figure 4A). After 8 weeks, the body weight of mice in the OVX group fed a normal diet (nCONT) was significantly higher than that of mice in the sham group (CONT) and mice in the OVX groups fed Sf and SfLlLm diets ($p < 0.01$; Figure 4B). OVX mice exhibited weight gain that is suppressed by 17β-estradiol, such as in the postmenopausal stage [33]. Mice administered SfLlLm had significantly lower body weight after 8 weeks than mice in the sham group. Next, ALP, pro-Col1A, and phosphate, markers for bone reconstruction, were measured in the separated plasma of mice using ELISA (Figure 4C–E). In Figure 4B, levels of ALP, pro-COL1α1, and phosphate in the nCONT were significantly higher than those of the sham and Sf- and SfLlLm groups after 8 weeks ($p < 0.05$). Molecules such as ALP, pro-COL1α1, and phosphate reflect the activity of osteoblasts and are important indices of osteogenesis [34]. Elevated levels of serum or plasma ALP, pro-COL1α1, and phosphate were found to be associated with an increase in osteoblast activity after OVX-induced osteoporosis [34,35]. Particularly, plasma levels of ALP and pro-COL1α1, as bone formation markers, were effectively reduced in the SfLlLm group when compared with those in the nCONT group (Figure 4C,D). Levels of phosphate, a bone-related mineral marker, were lower in the Sf group than in the SfLlLm group; however, this difference was not statistically significant (Figure 4E). The administration of VitK in mice fed a high-fat diet reportedly enhances bone formation indices and reduces bone resorption indices [36]. However, VitK supplementation did not exert any significant effect on bone metabolism in mice fed a normal diet [36]. These findings support the possibility that VitK, including MKs from SfLlLm produced by LAB, stimulates osteoblasts in OVX mice.

Bone is composed of outer bone comprising cortical bone (compact bone [80%]) and inner bone comprising trabecular bone (cancellous bone [20%]) [37]. Bone density tests are mainly performed in the trabecular bone because osteoporosis appears and progresses faster in trabecular bone than in cortical bone [38]. As shown in Figure 4F,G, trabecular bone parameters (cancellous bone volume and number of trabeculae) in the distal metaphyseal region of the femurs were significantly reduced by OVX in all treatment groups. SfLlLm-treated OVX mice exhibited higher cancellous bone volume (BV/TV; $2.76 \pm 0.00\ mm^3/mm^3$) than non-treated ($1.91 \pm 0.02\ mm^3/mm^3$) or Sf-treated OVX mice ($2.45 \pm 0.00\ mm^3/mm^3$) but lower than sham mice ($3.64 \pm 0.00\ mm^3/mm^3$; Figure 4G). The bone trabecular number level was recovered in OVX mice fed Sf- and SfLlLm diets ($1.04 \pm 0.02\ g/cm^2$) when compared with that in nCONT mice ($0.89 \pm 0.09\ g/cm^2$). Collectively, these results indicate that the SfLlLm diet may be a candidate for preventing and treating osteoporosis by improving bone formation. Recent evidence suggests that VitK2 (MKs) may regulate osteoblastogenesis and osteoclastogenesis via the NF-κB signal transduction pathway [27]. Bone remodeling is a lifelong process in which the volume of bone resorbed by osteoclasts is restored by bone-forming osteoblasts [39]. Among the various factors involved in the bone remodeling process, VitK derived from SfLlLm, that is, the primary focus of this study, could impact the regulation of inflammatory cytokines and osteoblast activation. In conclusion, we successfully produced long-chain VitK2 (MKs) from algae- and LAB (LlLm)-based fermentation and confirmed the anti-inflammatory and bone health benefits when compared with only Sf-based VitK forms. These results also suggest the possibility of cooperation between algae and LAB for nutrient fortification purposes in the food industry and as nutritional supplements. However, to fully demonstrate the therapeutic potential of VitK (PK and MK) from SfLlLm in promoting bone health, additional experiments are needed to confirm the efficacy of sargassum- or brown-algae-derived VitK by LAB in preclinical experiments.

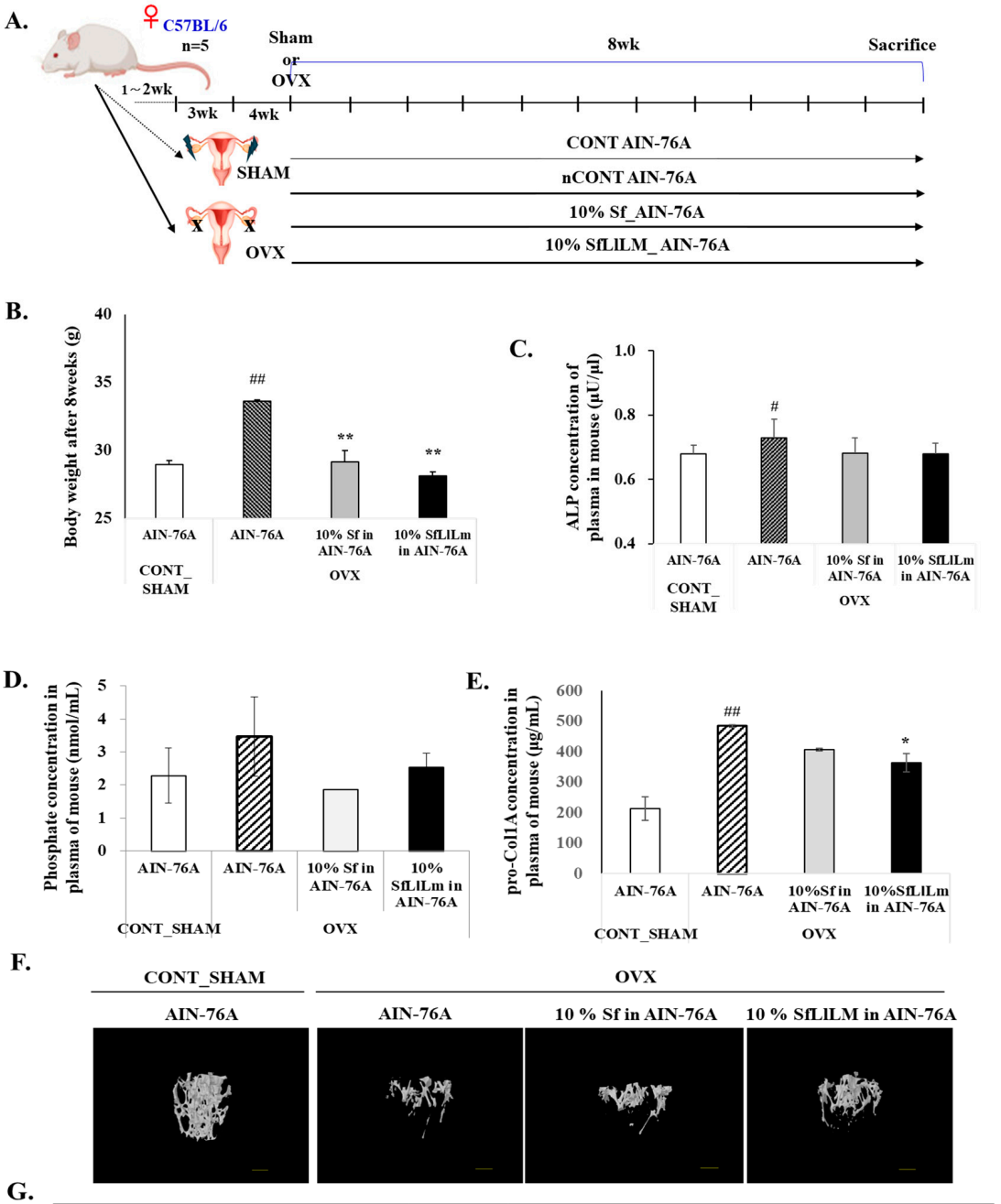

	CON	OVX		
FEED	**AIN-76A**	**AIN-76A**	**10% Sf in AIN-76A**	**10% SfLlLm in AIN-76A**
Cancellous bone volume (BV/TV; mm^3/mm^3)	3.64±0.01	01.91±0.02	2.45±0.00	2.76±0.00
Trabecular number (Tb.N; g/cm^2)	1.08±0.06	0.89±0.09	1.04±0.02	1.04±0.02

Figure 4. Osteogenic effect in ovariectomized (OVX) mouse: (**A**) Schematic diagram of the OVX mouse experiment. (**B**) Body weight changes over 8 weeks. (**C**–**E**) Immunoassay analysis for ALP (**C**), pro-Col1α1 (**D**), and phosphate (**E**) in plasma using ELISA. (**F**) Femur bone micro-computerized tomography analysis using micro-computed tomography analysis. (**G**) Bone structural parameters of trabecular bone (n = 5). Data are represented as the mean ± standard deviation of three independent experiments, # $p < 0.05$ vs. Control group, ## $p < 0.01$ vs. Control group, and * $p < 0.05$ and ** $p < 0.01$ vs. Control group. ALP, alkaline phosphatase; BV, bone volume; TV, tissue volume; Tb, trabecular thickness; pro-COL1A2, pro-collagen type I alpha 2 chain.

4. Conclusions

In conclusion, this study demonstrated that the potential anti-inflammatory and osteogenic benefits of VitK (PK, MK4, MK7, and MK9) derived from *S.fulvellum* fermented by *L. lactis* KCCM12759P and *L. mesenteroides* KCCM12756P using LPS-induced Raw264.7, MC3T3-E1 cells, and OVX mice. Therefore, SfLlLm including VitK may be a highly effective source of natural compounds for inflammation relief and bone health, where treatment options are limited and can have positive effects on the food and pharmaceutical industries.

Author Contributions: Y.S.: Conceptualization, Experiments, Investigation, Writing—original draft, Writing—revision and editing. H.-S.J.: Conceptualization, Experiments, Investigation, Writing—original draft, Writing—revision and editing. C.-G.K.: Data curation and visualization. Y.-E.C.: Conceptualization, Experimental Investigation, Formal Analysis. J.Y.; Conceptualization, Investigation. S.-M.H.: Conceptualization, Experimental Investigation, Supervision, Writing—original draft, Writing—revision and editing. All authors have read and agreed to the published version of the manuscript.

Funding: This research was funded by the Korea Institute of Marine Science and Technology Promotion (and) funded by the Ministry of Oceans and Fisheries, Korea (20220027).

Institutional Review Board Statement: All animal testing procedures were performed in accordance with the Andong University Small Animal Testing Guidelines and were approved by the Andong University Animal Care and Use Committee (Approval No.2021-2-0420-01-01).

Informed Consent Statement: Not applicable.

Data Availability Statement: The data presented in this study are available upon request from the corresponding author due to privacy restrictions.

Conflicts of Interest: The authors declare no conflicts of interest.

References

1. Liu, J.; Luthuli, S.; Wu, Q.; Wu, M.; Choi, J.I.; Tong, H. Pharmaceutical and nutraceutical potential applications of *Sargassum fulvellum*. *BioMed Res. Int.* **2020**, *2020*, 2417410. [CrossRef] [PubMed]
2. Wang, Y.; Liu, L.; Jin, Z.; Zhang, D. Microbial cell factories for green production of vitamins. *Front. Bioeng. Biotechnol.* **2021**, *9*, 661562. [CrossRef]
3. Croft, M.T.; Warren, M.J.; Smith, A.G. Algae need their vitamins. *Eukaryot Cell* **2006**, *5*, 1175–1183. [CrossRef] [PubMed]
4. Ren, L.; Peng, C.; Hu, X.; Han, Y.; Huang, H. Microbial production of vitamin K2: Current status and future prospects. *Biotechnol. Adv.* **2020**, *39*, 107453. [CrossRef] [PubMed]
5. Akbari, S.; Rasouli-Ghahroudi, A.A. Vitamin K and bone metabolism: A review of the latest evidence in preclinical studies. *BioMed Res. Int.* **2018**, *2018*, 4629383. [CrossRef] [PubMed]
6. Mahdinia, E.; Demirci, A.; Berenjian, A. Utilization of glucose-based medium and optimization of *Bacillus subtilis* natto growth parameters for vitamin K (menaquinone-7) production in biofilm reactors. *Biocatal. Agric. Biotechnol.* **2018**, *13*, 219–224. [CrossRef]
7. Chollet, M.; Guggisberg, D.; Portmann, R.; Risse, M.-C.; Walther, B. Determination of menaquinone production by *Lactococcus* spp. and propionibacteria in cheese. *Int. Dairy J.* **2017**, *75*, 1–9. [CrossRef]
8. Hojo, K.; Watanabe, R.; Mori, T.; Taketomo, N. Quantitative measurement of tetrahydromenaquinone-9 in cheese fermented by propionibacteria. *J. Dairy Sci.* **2007**, *90*, 4078–4083. [CrossRef]
9. Booth, S.L. Roles for vitamin K beyond coagulation. *Annu. Rev. Nutr.* **2009**, *29*, 89–110. [CrossRef] [PubMed]
10. Ferland, G. Vitamin K and the nervous system: An overview of its actions. *Adv. Nutr.* **2012**, *3*, 204–212. [CrossRef]
11. Shiraki, M.; Tsugawa, N.; Okano, T. Recent advances in vitamin K-dependent Gla-containing proteins and vitamin K nutrition. *Osteoporos Sarcopenia* **2015**, *1*, 22–38. [CrossRef]
12. Willems, B.A.; Vermeer, C.; Reutelingsperger, C.P.; Schurgers, L.J. The realm of vitamin K dependent proteins: Shifting from coagulation toward calcification. *Mol. Nutr. Food Res.* **2014**, *58*, 1620–1635. [CrossRef] [PubMed]
13. Villa, J.K.D.; Diaz, M.A.N.; Pizziolo, V.R.; Martino, H.S. Effect of vitamin K in bone metabolism and vascular calcification: A review of mechanisms of action and evidences. *Crit. Rev. Food Sci. Nutr.* **2017**, *57*, 3959–3970. [CrossRef]
14. Capozzi, A.; Scambia, G.; Lello, S. Calcium, vitamin D, vitamin K2, and magnesium supplementation and skeletal health. *Maturitas* **2020**, *140*, 55–63. [CrossRef]
15. Wegmann, U.; O'Connell-Motherway, M.; Zomer, A.; Buist, G.; Shearman, C.; Canchaya, C.; Ventura, M.; Goesmann, A.; Gasson, M.J.; Kuipers, O.P.; et al. Complete genome sequence of the prototype lactic acid bacterium *Lactococcus lactis subsp. cremoris* MG1363. *J. Bacteriol.* **2007**, *189*, 3256–3270. [CrossRef]
16. Watthanasakphuban, N.; Virginia, L.J.; Haltrich, D.; Peterbauer, C. Analysis and reconstitution of the menaquinone biosynthesis pathway in *Lactiplantibacillus plantarum* and *Lentilactibacillus buchneri*. *Microorganisms* **2021**, *9*, 1476. [CrossRef] [PubMed]

17. Lee, S.H.; Hong, S.M.; Sung, M.J. Inhibitory effect of fermented spanish extract on inorganic phosphate-induced vascular calcification in ex vivo aortic rings. *J. Korean Soc. Food Cult.* **2022**, *37*, 248–255. [CrossRef]
18. Narla, R.R.; Ott, S.M. Bones and the sex hormones. *Kidney Int.* **2018**, *94*, 239–242. [CrossRef] [PubMed]
19. Cheng, C.H.; Chen, L.R.; Chen, K.H. Osteoporosis due to hormone imbalance: An overview of the effects of estrogen deficiency and glucocorticoid overuse on bone turnover. *Int. J. Mol. Sci.* **2022**, *23*, 1376. [CrossRef]
20. Arboleya, L.; Castañeda, S. Osteoinmu nología: El estudio de la relación entre el sistema inmune y el tejido óseo. *Reumatol. Clin.* **2013**, *9*, 303–315. [CrossRef]
21. Castañeda, S.; Garcés-Puentes, M.V.; Bernad Pineda, M. Pathophysiology of osteoporosis in chronic inflammatory joint diseases. *Rev. Osteoporos. Metab. Miner.* **2021**, *13*, 32–38. [CrossRef]
22. Manoury, E.; Jourdon, K.; Boyaval, P.; Fourcassié, P. Quantitative measurement of vitamin K2 (menaquinones) in various fermented dairy products using a reliable high-performance liquid chromatography method. *J. Dairy Sci.* **2013**, *96*, 1335–1346. [CrossRef] [PubMed]
23. Sim, Y.J.; Seo, H.J.; Kim, D.; Lee, S.H.; Kwon, J.H.; Kwun, I.S.; Jung, C.; Kim, J.I.; Lim, J.H.; Kim, D.K. The effect of apple-derived nanovesicles on the osteoblastogenesis of osteoblastic MC3T3-E1 cells. *J. Med. Food* **2023**, *26*, 49–58. [CrossRef] [PubMed]
24. Hwang, J.H.; Park, Y.S.; Kim, H.S.; Kim, D.; Lee, S.H.; Lee, C.H.; Lee, S.H.; Kim, J.E.; Lee, S.; Kim, H.M. Yam-derived exosome-like nanovesicles stimulate osteoblast formation and prevent osteoporosis in mice. *JCR* **2023**, *355*, 184–198. [CrossRef]
25. Morishita, T.; Tamura, N.; Makino, T.; Kudo, S. Production of menaquinones by lactic acid bacteria. *J. Dairy Sci.* **1999**, *82*, 1897–1903. [CrossRef]
26. Kimball, J.S.; Johnson, J.P.; Carlson, D.A. Oxidative stress and osteoporosis. *J. Bone Joint Surg.* **2021**, *103*, 1451–1461. [CrossRef]
27. Yamaguchi, M.; Weitzmann, M.N. Vitamin K2 stimulates osteoblastogenesis and suppresses osteoclastogenesis by suppressing NF-kappaB activation. *Int. J. Mol. Med.* **2011**, *27*, 3–14. [CrossRef]
28. Hara, K.; Akiyama, Y.; Nakamura, T.; Murota, S.; Morita, I. The inhibitory effect of vitamin K2 (menatetrenone) on bone resorption may be related to its side chain. *Bone* **1995**, *16*, 179–184. [CrossRef]
29. Beck, G.R., Jr.; Zerler, B.; Moran, E. Phosphate is a specific signal for induction of osteopontin gene expression. *Proc. Natl. Acad. Sci. USA* **2000**, *97*, 8352–8357. [CrossRef]
30. Nizet, A.; Cavalier, E.; Stenvinkel, P.; Haarhaus, M.; Magnusson, P. Bone alkaline phosphatase: An important biomarker in chronic kidney disease–mineral and bone disorder. *Clin. Chim. Acta* **2020**, *501*, 198–206. [CrossRef]
31. Bernar, A.; Gebetsberger, J.V.; Bauer, M.; Streif, W.; Schirmer, M. Optimization of the alizarin red S assay by enhancing mineralization of osteoblasts. *Int. J. Mol. Sci.* **2022**, *24*, 723. [CrossRef] [PubMed]
32. Zhang, Y.L.; Yin, J.H.; Ding, H.; Zhang, W.; Zhang, C.Q.; Gao, Y.S. Protective effect of VK2 on glucocorticoid-treated MC3T3-E1 cells. *Int. J. Mol. Med.* **2017**, *39*, 160–166. [CrossRef] [PubMed]
33. Ornoy, A.; Giron, S.; Aner, R.; Goldstein, M.; Boyan, B.D.; Schwartz, Z. Gender dependent effects of testosterone and 17β-estradiol on bone growth and modelling in young mice. *Bone Min.* **1994**, *24*, 43–58. [CrossRef] [PubMed]
34. Hong, S.; Cha, K.H.; Park, J.H.; Jung, D.S.; Choi, J.H.; Yoo, G.; Nho, C.W. Cinnamic acid suppresses bone loss via induction of osteoblast differentiation with alteration of gut microbiota. *J. Nutr. Biochem.* **2022**, *101*, 108900. [CrossRef]
35. Raisz, L.G. Pathogenesis of osteoporosis: Concepts, conflicts, and prospects. *J. Clin. Investig.* **2005**, *115*, 3318–3325. [CrossRef]
36. Kim, M.; Na, W.; Sohn, C. Vitamin K1 (phylloquinone) and K2 (menaquinone-4) supplementation improves bone formation in a high-fat diet-induced obese mice. *J. Clin. Biochem. Nutr.* **2013**, *53*, 108–113. [CrossRef] [PubMed]
37. Clarke, B. Normal bone anatomy and physiology. *Clin. J. Am. Soc. Nephrol.* **2008**, *3*, 131–139. [CrossRef]
38. Guglielmi, G.; Muscarella, S.; Bazzocchi, A. Integrated imaging approach to osteoporosis: State-of-the-art review and update. *Radiographics* **2011**, *31*, 1343–1364. [CrossRef]
39. Amarasekara, D.S.; Yun, H.; Kim, S.; Lee, N.; Kim, H.; Rho, J. Regulation of osteoclast differentiation by cytokine networks. *Immune Netw.* **2018**, *18*, e8. [CrossRef]